THE JOURNAL OF BIOLOGICAL CHEMISTRY VOL. 290, NO. 43, pp. 26328–26338, October 23, 2015

Phosphorylation of Serine 402 Regulates RacGAP Protein Activity of FilGAP Protein*

Received for publication, May 21, 2015, and in revised form, August 27, 2015 Published, JBC Papers in Press, September 10, 2015, DOI 10.1074/jbc.M115.666875

Yuji Morishita, Koji Tsutsumi, and Yasutaka Ohta[1]

From the Division of Cell Biology, Department of Biosciences, School of Science, Kitasato University, 1-15-1 Kitasato, Sagamihara, Minami-ku, Kanagawa 252-0373, Japan

Background: FilGAP is a Rac GTPase-activating protein, but regulation via phosphorylation has not been previously characterized.
Results: Phosphorylation of FilGAP at serine 402 is necessary to activate FilGAP to suppress cell spreading on fibronectin.
Conclusion: Serine 402 is a critical phosphorylation site to regulate FilGAP activity.
Significance: This study showed that regulation of FilGAP by phosphorylation may play a role in integrin-mediated cell adhesion on fibronectin.

FilGAP is a Rho GTPase-activating protein (GAP) that specifically regulates Rac. FilGAP is phosphorylated by ROCK, and this phosphorylation stimulates its RacGAP activity. However, it is unclear how phosphorylation regulates cellular functions and localization of FilGAP. We found that non-phosphorylatable FilGAP (ST/A) mutant is predominantly localized to the cytoskeleton along actin filaments and partially co-localized with vinculin around cell periphery, whereas phosphomimetic FilGAP (ST/D) mutant is diffusely cytoplasmic. Moreover, phosphorylated FilGAP detected by Phos-tag is also mainly localized in the cytoplasm. Of the six potential phosphorylation sites in FilGAP tested, only mutation of serine 402 to alanine (S402A) resulted in decreased cell spreading on fibronectin. FilGAP phosphorylated at Ser-402 is localized to the cytoplasm but not at the cytoskeleton. Although Ser-402 is highly phosphorylated in serum-starved quiescent cells, dephosphorylation of Ser-402 is accompanied with the cell spreading on fibronectin. Treatment of the cells expressing wild-type FilGAP with calyculin A, a Ser/Thr phosphatase inhibitor, suppressed cell spreading on fibronectin, whereas cells transfected with FilGAP S402A mutant were not affected by calyculin A. Expression of constitutively activate Arf6 Q67L mutant stimulated membrane blebbing activity of both non-phosphorylatable (ST/A) and phosphomimetic (ST/D) FilGAP mutants. Conversely, depletion of endogenous Arf6 suppressed membrane blebbing induced by FilGAP (ST/A) and (ST/D) mutants. Our study suggests that Arf6 and phosphorylation of FilGAP may regulate FilGAP, and phosphorylation of Ser-402 may play a role in the regulation of cell spreading on fibronectin.

Rho family small GTPases (Rho GTPases) are involved in the control of actin cytoskeleton and membrane dynamics and play essential roles in many cellular functions such as cell adhesion, cell migration, and vesicle trafficking (1–6). Rho GTPases function as molecular switches in cells. They exist in either an inactive GDP-bound state or an active GTP-bound state; in the active state, they stimulate downstream effectors. This cycle is mainly regulated by two classes of proteins. Guanine nucleotide exchange factors activate Rho GTPases by loading GTP, whereas GTPase-activating proteins (GAPs)[2] facilitate the inactivation of Rho GTPases by stimulating their intrinsic GTPase activity (7–11).

FilGAP is a Rac-specific GAP that suppresses Rac-dependent lamellipodia formation and cell spreading (12–20). Phosphorylation of FilGAP by Rho/Rho-associated protein kinase (ROCK) stimulates its Rac GAP activity (12). Depletion of endogenous FilGAP by siRNA induces a Rac-driven elongated mesenchymal morphology. Conversely, overexpression of FilGAP induces membrane blebbing and a rounded amoeboid morphology contingent upon Rho/ROCK-dependent phosphorylation of FilGAP (18). Thus, FilGAP mediates antagonism of Rac by Rho, which suppresses the elongated mesenchymal morphology and promotes rounded amoeboid migration (18, 19, 21, 22).

Although Rho/ROCK-dependent phosphorylation of FilGAP stimulates its RacGAP activity *in vivo*, such phosphorylation has no effect on the catalytic activity of FilGAP *in vitro* (12). In this report we present evidence that phosphorylation of FilGAP may regulate its subcellular localization. We also show that Ser-402 is an important phosphorylation site for the regulation of FilGAP activity.

Experimental Procedures

Proteins and Plasmids—The HA-tagged FilGAP (wild-type, ST/D, ST/A, S391A, S402A, S413A, S415A, S437A, and T452A) constructs in pCMV5 vector were described previously (12, 18). The HA-tagged Arf6 (Q67L) construct in the pcDNA vector was provided by Dr. Nakayama (Kyoto University, Kyoto, Japan). *Arf6* siRNA-resistant construct (HA-Arf6 $Q67L^R$) was

* This work was supported by grants-in-aid for Scientific Research from the Japan Society for the Promotion of Science and the Ministry of Education, Culture, Sports, Science, and Technology of Japan, a Grant for All Kitasato Project Study, and a Kitasato University Research Grant for Young Researchers. The authors declare that they have no conflicts of interest with the contents of this article.
[1] To whom correspondence should be addressed. Tel.: 81-42-778-9401; Fax: 81-42-778-9401; E-mail: yohta@kitasato-u.ac.jp.

[2] The abbreviations used are: GAP, GTPase-activating protein; ROCK, Rho/Rho-associated protein kinase; ANOVA, analysis of variance.

generated by introducing 5 silent point mutations to siRNA targeting sequence (nucleotides 73–97). The final mutant was changed into ^{73}GGTAAGACTACAATTCTTTACAAAT^{97} by PCR. The FLAG-tagged FilGAP (wild-type, ST/D, and ST/A) constructs in pCMV5 vector were described previously (20).

Cell Culture—HEK 293, HeLa, COS-7, and MDA-MB-231 cells were grown at 37 °C in DMEM (Sigma) supplemented with 10% (v/v) fetal bovine serum (FBS) and 50 units/ml penicillin/streptomycin at 37 °C. The human melanoma cell lines A7 were grown in minimum Eagle's medium (Sigma) supplemented with 2% FBS, 8% newborn calf serum, 50 units/ml penicillin/streptomycin, and 50 μg/ml Geneticin at 37 °C. For transfection, cells were transfected with plasmid DNA using Lipofectamine 2000 as described by the manufacturers (Invitrogen). Immunofluorescent staining was performed as described (12). Briefly, cells plated on coverslips were fixed in 3.7% formaldehyde, permeabilized in 0.5% Triton X-100, and stained with anti-HA or other antibodies. For cytoskeletal staining, cells were washed once by PHEM buffer (20 mM PIPES, 2 mM $MgCl_2$, 50 mM KCl, 5 mM EGTA, 5 mM DTT, and 1 mM ATP), permeabilized in PHEM buffer containing 0.5% Triton X-100 for 2 min, and then fixed in PHEM buffer containing 3.7% formaldehyde at room temperature. For visualization of F-actin, cells were stained with Alexa Fluor 568-conjugated phalloidin in PBS for 1 h. Cells were observed under an Olympus IX81 fluorescence microscope (Olympus, Tokyo, Japan). Images were acquired by a charge-coupled device camera (ORCA-ER; Hamamatsu photonics, Hamamatsu, Japan) with constant exposure time (300 ms for transfected cells and 1 s for detecting endogenous protein) and analyzed by MetaMorph software (Molecular Devices, Sunnyvale, CA).

Antibodies—Mouse anti-HA (12CA5) antibody was purchased from Roche Applied Science. Mouse monoclonal anti-α-tubulin and anti-vinculin antibodies were purchased from Sigma. Mouse monoclonal anti-vimentin antibody was purchased from Dako Cytomation. Mouse monoclonal anti-Arf6 antibody was purchased from Santa Cruz Biotechnology. Polyclonal antibodies against FilGAP were raised in rabbits and purified as described previously (20). Secondary antibodies conjugated to Alexa Fluor 488 or 568 and Alexa Fluor 568-phalloidin were also purchased from Invitrogen. Rabbit anti-Ser(P)-402 FilGAP polyclonal antibody was directed against amino acid residues 397–407 (CGSKTNpSPKNSV) of human FilGAP protein. The peptide was coupled through cysteine at the NH_2-terminal residue to keyhole limpet hemocyanin (KLH) and was used to raise the antiserum. The antiserum specific to Ser(P)-402 FilGAP was affinity-purified with the immobilized peptides. The first column contains phosphorylated peptides (CGSKTNpSPKNSV), and the second column holds non-phosphorylated peptide (CGSKTNSPKNSV). The animal experiments were carried out in strict accordance with the protocols approved by committee of Kitasato University (No.SA1010). All efforts were made to minimize animal suffering.

Cell Spreading Assay—A cell spreading assay was performed as described (12). Briefly, quiescent cells were trypsinized and suspended in serum-free minimum Eagle's medium containing 0.2% BSA (Calbiochem) and incubated as a suspension for 1 h at 37 °C. Cells were then plated on fibronectin-coated cover slips and incubated for the indicated time periods at 37 °C. The cells were fixed and processed for immunofluorescence staining. For immunoblotting, cells were washed twice with 2 ml of PBS and suspended with 200 μl of lysis buffer (radioimmune precipitation assay buffer) containing 50 mM Tris-HCl (pH 7.4), 500 mM NaCl, 0.5% Triton X-100, 0.5% sodium deoxycholate, 0.1% SDS, 1 mM EDTA, 1 mM sodium orthovanadate, 30 mM sodium pyrophosphate, and 50 mM sodium fluoride with protease inhibitors. The cell lysates were precleared, the supernatants were collected and subjected to SDS-PAGE, and proteins were detected by immunoblot using anti-HA or anti-Ser(P)-402 antibody.

Subcellular Fractionation—Cells transfected with HA-FilGAP were washed twice with 2 ml of PBS and lysed in 120 μl of PHEM buffer containing 0.5% Triton X-100 with protease inhibitors. Cell suspensions were collected with a rubber policeman and centrifuged at 21,600 $\times$ *g* for 3 min. Supernatant fluids were removed, and the pellets were suspended in 120 μl of PBS containing 1% SDS. Fractions were subjected to SDS-PAGE, and proteins were detected by immunoblot using anti-HA antibody. The relative amount of HA-FilGAP protein in the cytoskeleton and supernatant was quantitated from digitized images of immunoblots by using the Image J analysis program.

Dephosphorylation Assay—HA-FilGAP protein was immunoprecipitated using anti-HA-agarose beads from HEK cells transfected with pCMV5-HA-FilGAP. After immunoprecipitation, the anti-HA beads were washed once with PBS and then three times with calf intestine alkaline phosphatase reaction buffer (TaKaRa) containing 10 mM Tris-HCl (pH 9.0) and 1 mM $MgCl_2$. The precipitates were resuspended in 40 μl of calf intestine alkaline phosphatase buffer with or without 20 units of calf intestine alkaline phosphatase (TaKaRa). The beads were incubated for 30 min at 37 °C in the presence or absence of phosphatase inhibitors containing 10 mM sodium fluoride, 2 mM β-glycerophosphate, and 2 mM sodium pyrophosphate. The reaction was terminated by adding 10 μl of 1% SDS, boiled for 5 min, and centrifuged. The supernatants were collected and subjected to SDS-PAGE. Bound-proteins were detected by immunoblot using anti-HA or anti-Ser(P)-402 antibody. For phosphatase inhibitor (calyculin A) treatment, A7 cells transfected with HA-FilGAP were serum-starved. The quiescent cells were incubated with 10 μM calyculin A (Cell Signaling) for 30 min at 37 °C. After treatment, the cells were washed 3 times with 2 ml of PBS, lysed by 120 μl of lysis buffer (radioimmune precipitation assay buffer) containing 50 mM Tris-HCl (pH 7.4), 500 mM NaCl, 0.5% Triton X-100, 0.5% sodium deoxycholate, 0.1% SDS, 1 mM EDTA, 1 mM sodium orthovanadate, 30 mM sodium pyrophosphate, and 50 mM sodium fluoride with protease inhibitors, and centrifuged at 200,000 $\times$ *g* for 20 min. The supernatants were collected and subjected to SDS-PAGE. Bound proteins were detected by immunoblot using anti-HA or anti-Ser(P)-402 antibody.

Phos-tag SDS-PAGE—Phos-tag SDS-PAGE using a 6% polyacrylamide gel containing 25 μM Phos-tag acrylamide (Wako Chemicals) and 100 μM $MnCl_2$ was also carried out according to the manufacturer's instructions.

Statistical Analysis—The statistical significance was assessed by two-tailed unpaired Student's *t* test or one-way analysis of variance (ANOVA).

RNA Interference—siRNA oligonucleotides were purchased from Invitrogen. The targeting sequence of *Arf6* was 5′-GGCAAGACAACAAUCCUGUACAAGU-3′. The targeting sequence of *FilGAP* was 5′-CAGUGGUAAAUUACAACCUCCUCAA-3′. A7 cells were transfected with *Arf6* siRNA using Lipofectamine 2000. COS-7 cells were transfected with *FilGAP* siRNA using Lipofectamine 2000. Forty-eight hours after transfection, the levels of each protein were measured by Western blot analysis using anti-Arf6 or anti-FilGAP antibody.

Results

Phosphorylation of FilGAP Regulates Its Subcellular Localization—We have shown previously that a FilGAP mutant with all potential phosphorylation sites mutated to alanine (ST/A) failed to function as a RacGAP in cells, whereas a FilGAP mutant with all potential phosphorylation sites mutated to phosphomimetic aspartic acid (ST/D) suppressed Rac-driven lamellae formation *in vivo*. However, it is unclear how phosphorylation regulates FilGAP. To determine whether phosphorylation regulates subcellular localization of FilGAP, we compared the localization of non-phosphorylatable (ST/A) and phosphomimetic (ST/D) FilGAP mutants. We found >40% of the ST/A mutant in the Triton X-100 insoluble fraction (*i.e.* the cytoskeleton), whereas <20% of the ST/D mutant was found in this fraction (Fig. 1, *A* and *B*). We next analyzed the localization of phosphorylated FilGAP using Phos-tag SDS-PAGE. Phosphorylated proteins can be detected by their delayed migration in Phos-tag SDS-PAGE gels (23, 24). When FilGAP protein immunoprecipitated from transfected cells (HA-FilGAP) was resolved by Phos-tag SDS-PAGE, the migration of non-phosphorylatable FilGAP (ST/A) protein was much faster than that of wild-type FilGAP protein (Fig. 1*C*). This suggests that the serine and threonine residues mutated to alanine are major phosphorylation sites *in vivo*. Moreover, although phosphorylated FilGAP was mainly recovered in the Triton X-100 soluble fraction, the mobility of non-phosphorylatable FilGAP (ST/A) did not differ between Triton X-100 soluble and insoluble fractions (Fig. 1*C*). To further demonstrate that phosphorylation is responsible for release of FilGAP from the cytoskeleton, we determined the effect of calyculin A, an inhibitor of protein phosphatase 2A and protein phosphatase 1. As shown in Fig. 1, *D* and *E*, treatment of the cells with calyculin A reduced the amount of HA-FilGAP localized to the cytoskeleton. Endogenous FilGAP was also released from the cytoskeleton after treatment with calyculin A (Fig. 1, *F* and *G*).

After transient transfection of cells with HA-FilGAP constructs, wild-type FilGAP localized with actin filaments (Fig. 2). Wild-type FilGAP was also localized to the Triton X-100 insoluble cytoskeleton and co-localized with vinculin at the cell peripheries (Fig. 3). Both the non-phosphorylatable FilGAP (ST/A) mutant and the phosphomimetic FilGAP (ST/D) mutant localized with actin filaments and vinculin at the cell peripheries. However, although the ST/A mutant localized to the cytoskeleton with actin filaments and vinculin, little ST/D mutant was detected at the cytoskeleton (Figs. 2 and 3). These

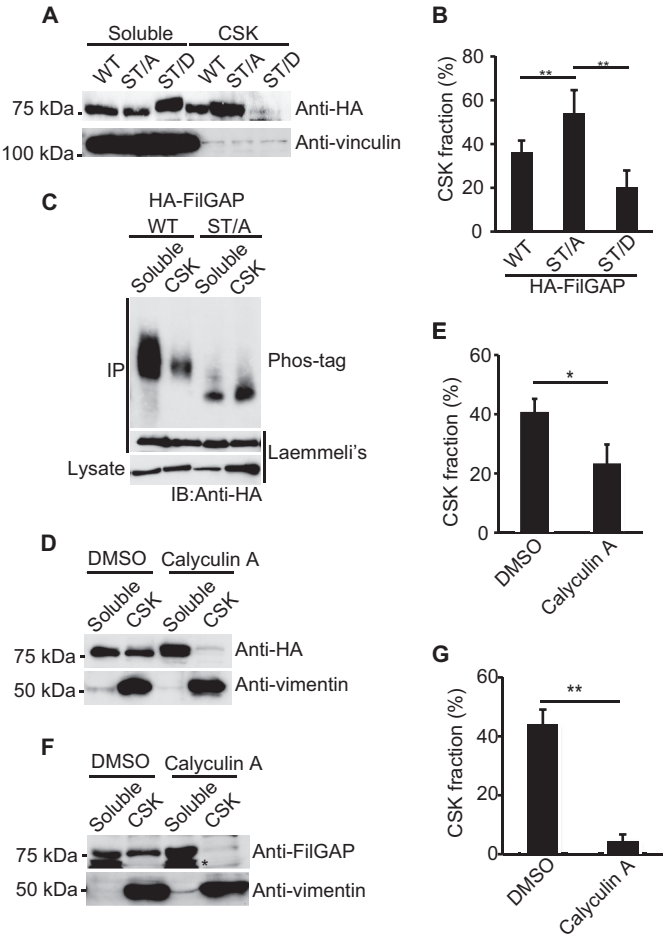

FIGURE 1. **Phosphorylation of FilGAP regulates its subcellular localization.** *A*, HEK cells were transfected with HA-tagged wild-type FilGAP, non-phosphorylatable ST/A, or phosphomimetic ST/D FilGAP mutant. The cells were lysed and Triton-solubilized, and insoluble cytoskeletal (*CSK*) fractions were prepared. Samples of each fraction were immunoblotted with anti-HA antibody to detect HA-FilGAP. Vinculin was used as a loading control. *B*, the relative amounts of HA-FilGAP in the cytoskeletons were quantitated from digitized images of autoradiograms of immunoblots by using Image J program. Each value represents the percentage of total and the mean ± S.E. ($n = 7$). **, $p < 0.01$. Statistical significance was determined by one-way ANOVA. *C*, human melanoma A7 cells were transfected with HA-tagged wild-type FilGAP or non-phophorylatable (ST/A) FilGAP mutant. The cells were lysed and Triton-solubilized, and insoluble cytoskeletal fractions were prepared. HA-FilGAP proteins were immunoprecipitated (*IP*) from each fraction and subjected to Phos-tag SDS-PAGE (*upper lane*) or Laemmli SDS-PAGE (*lower panel*) and detected by immunoblot (*IB*) using anti-HA antibody. *D*, A7 cells were transfected with HA-FilGAP (wild type) and serum-starved. Quiescent cells were incubated with DMSO or 10 nM calyculin A for 30 min at 37 °C. Then the cells were lysed and Triton-solubilized, and insoluble cytoskeletal fractions were prepared. Samples of each fraction were immunoblotted with anti-HA antibody. Vimentin was used as a marker of cytoskeletal protein. *E*, the relative amounts of HA-FilGAP in the cytoskeleton were quantitated from digitized images of autoradiograms of immunoblots by using Image J program. Each value represents the percentage of total and the mean ± S.E. of triplicate determinations. *, $p < 0.05$. Statistical significance was determined by Student's *t* test. *F*, human breast adenocarcinoma MDA-MB-231 cells were serum-starved. Quiescent cells were incubated with DMSO or 10 nM calyculin A for 60 min at 37 °C. Then the cells were lysed and Triton-solubilized, and insoluble cytoskeletal fractions were prepared. Samples of each fraction were immunoblotted with anti-FilGAP antibody. Vimentin was used as a marker of cytoskeletal protein. *G*, the relative amounts of endogenous FilGAP in the cytoskeleton were quantitated from digitized images of autoradiograms of immunoblots by using Image J program. Each value represents the percentage of total and the mean ± S.E. of triplicate determinations. **, $p < 0.005$. Statistical significance was determined by Student's *t* test.

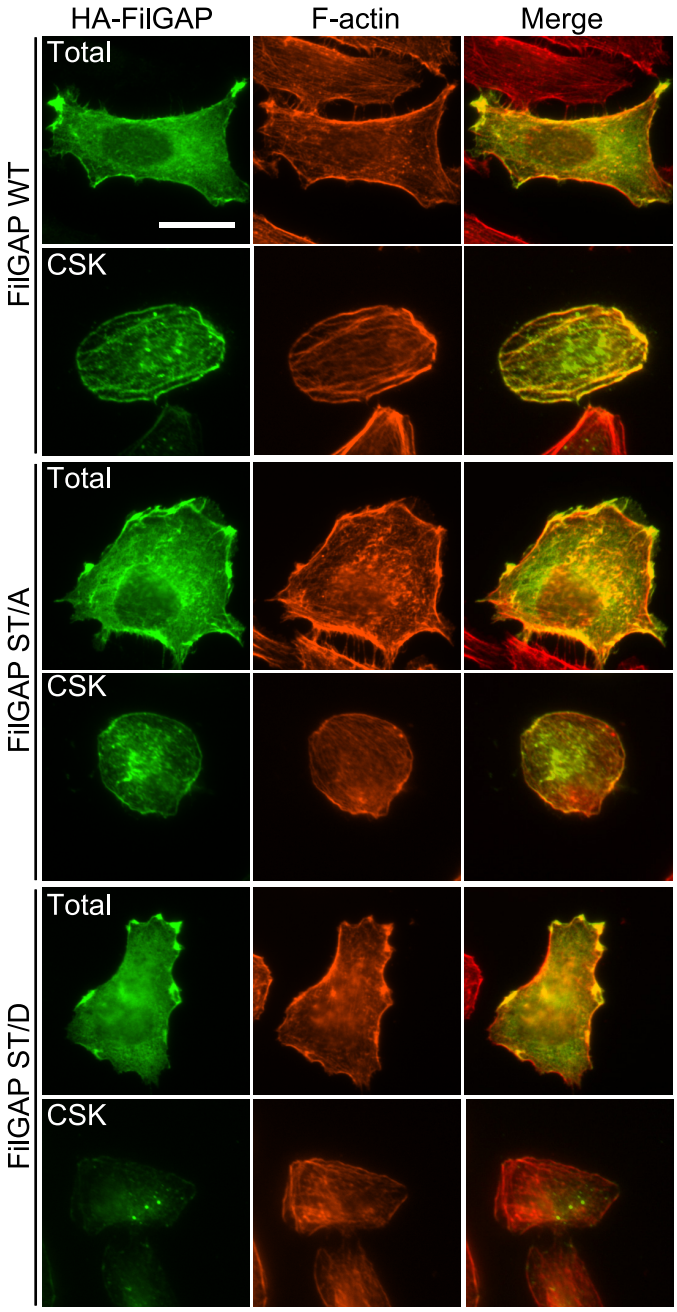

FIGURE 2. **Subcellular localization of FilGAP.** A7 cells were transfected with HA-tagged wild-type (*WT*) FilGAP, non-phosphorylatable (*ST/A*), or phosphomimetic (*ST/D*) FilGAP mutant. The cells were fixed after treatment with cytoskeletal (*CSK*) or without (*Total*) 0.5% Triton X-100. HA-FilGAP (*green*) and F-actin (*red*) were localized by staining the cells with anti-HA antibody and Alexa Fluor-phalloidin. Merged fluorescent images are also shown. *Scale bar*, 20 μm.

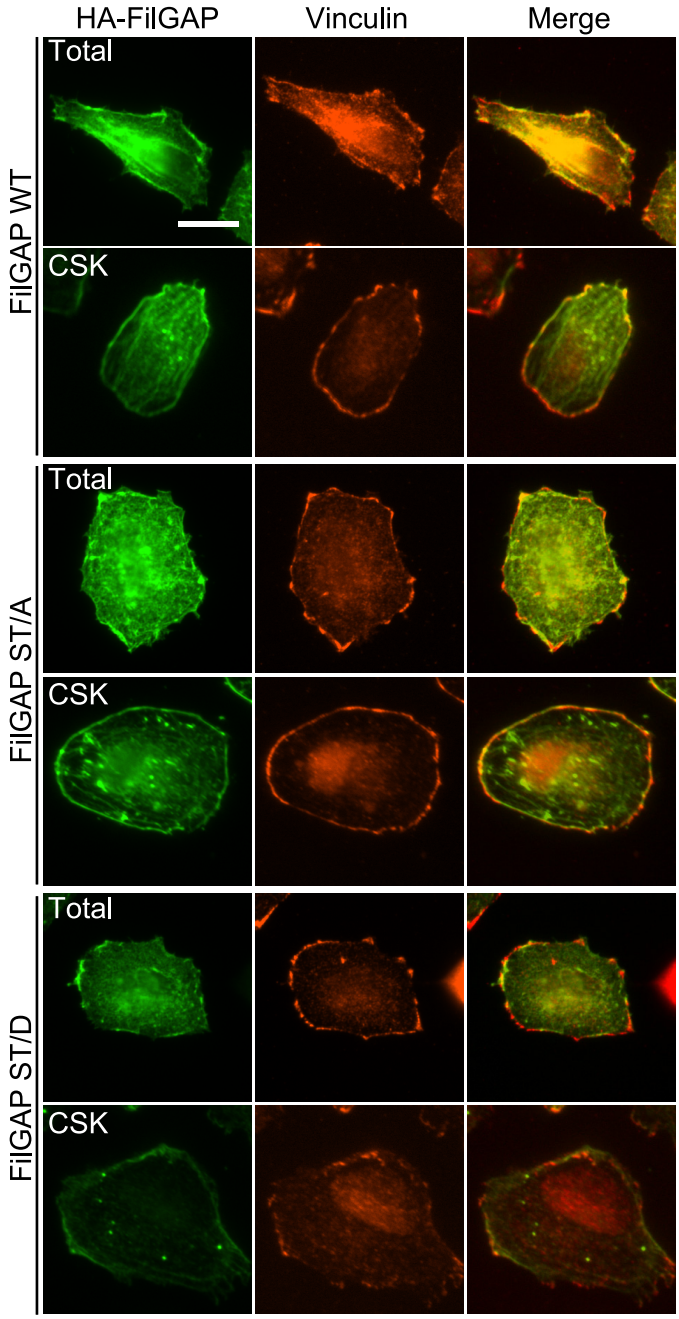

FIGURE 3. **Subcellular localization of FilGAP.** A7 cells were transfected with HA-tagged wild-type (*WT*) FilGAP, non-phosphorylatable (*ST/A*), or phosphomimetic (*ST/D*) FilGAP mutant. The cells were fixed after treatment with cytoskeletal (*CSK*) or without (*Total*) 0.5% Triton X-100. HA-FilGAP (*green*) and vinculin (*red*) were localized by staining the cells with anti-HA and anti-vinculin antibodies. Merged fluorescent images are also shown. *Scale bar*, 20 μm.

results suggest that non-phosphorylated FilGAP may associate with the cytoskeleton and that phosphorylation of FilGAP at critical residues may induce translocation of FilGAP from the cytoskeleton to the cytoplasm, which may be required for activation of FilGAP.

Determination of the Critical Phosphorylation Site of FilGAP—A7 cells that were plated on fibronectin-coated coverslips adhered and then started to spread within 20 min (Fig. 4*A*) (12). Forced expression of wild-type FilGAP or the phosphomimetic FilGAP (ST/D) mutant abolished cell spreading, whereas overexpression of the non-phosphorylatable FilGAP (ST/A) mutant enhanced initial cell spreading on fibronectin (Fig. 4*A*). The spread area occupied by cells expressing the ST/A mutant-expressing cells was larger than that occupied by cells expressing wild-type FilGAP or the ST/D mutant (Fig. 4*B*). Therefore, phosphorylation of FilGAP is required for efficient suppression of cell spreading on fibronectin.

We used the cell-spreading assay to determine which phosphorylation site of FilGAP is critical for its activation. Among the FilGAP mutants with one potential phosphorylation site

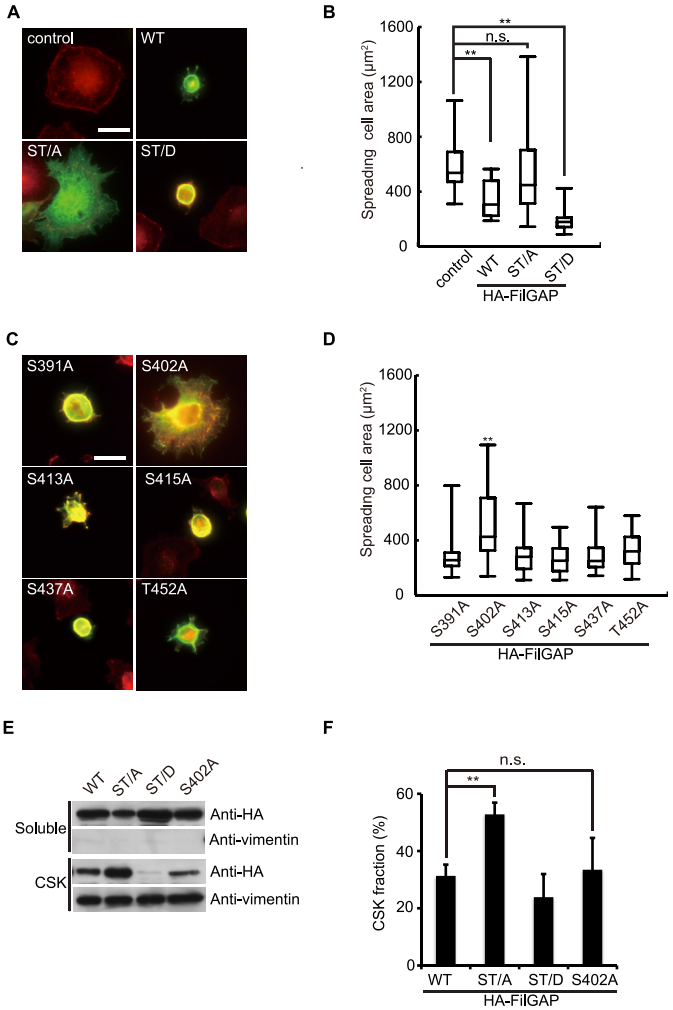

FIGURE 4. **Identification of Serine 402 of FilGAP as a critical phosphorylation site to regulate FilGAP activity.** *A*, HeLa cells were transfected without (control) or with HA-tagged wild-type FilGAP (*WT*), non-phosphorylatable (*ST/A*), or phosphomimetic (*ST/D*) FilGAP mutant and serum-starved. The quiescent cells were trypsinized, and cells in suspension were plated on coverslips coated with fibronectin and fixed 20 min after plating. Cells were stained with anti-HA antibody for HA-FilGAP (*green*) and Alexa Fluor-phalloidin for F-actin (*red*). Representative merged images of cells are shown. *Scale bar*, 50 μm. *B*, the surface area of spreading cells 20 min after plating was calculated and plotted as the mean ± S.E. ($n = 3$). >50 cells were analyzed in each experiment. **, $p < 0.01$. Statistical significance was determined by one-way ANOVA. *n.s.*, not significant. *C*, HeLa cells were transfected with HA-tagged FilGAP mutants and serum-starved. The quiescent cells were trypsinized, and cells in suspension were plated on coverslips coated with fibronectin and fixed 20 min after plating. Cells were stained with anti-HA antibody for HA-FilGAP mutants (*green*) and Alexa Fluor-phalloidin for F-actin (*red*). Representative of merged images of cells are shown. *Scale bar*, 50 μm. *D*, the surface area of spreading cells 20 min after plating was calculated and plotted as the mean ± S.E. ($n = 3$). >50 cells were analyzed in each experiment. **, $p < 0.01$. Statistical significance was determined by one-way ANOVA. *E*, A7 cells were transfected with HA-FilGAP constructs (wild-type, ST/A, ST/D, or S402A). The cells were lysed and Triton-solubilized, and insoluble cytoskeletal (*CSK*) fractions were prepared. Samples of each fraction were immunoblotted with anti-HA antibody to detect HA-FilGAP. Vimentin was used as a marker of cytoskeletal protein. *F*, the relative amounts of HA-FilGAP in the cytoskeletons were quantitated from digitized images of autoradiograms of immunoblots by using Image J program. Each value represents the percentage of total and the mean ± S.E. ($n = 3$). **, $p < 0.01$. Statistical significance was determined by Student's *t* test.

mutated to alanine, only the mutant with Ser-402 mutated to alanine (S402A) stimulated initial cell spreading on fibronectin (Fig. 4, *C* and *D*). Thus, phosphorylation of Ser-402 is required for activation of FilGAP.

We next determined whether phosphorylation of FilGAP at Ser-402 regulates localization of FilGAP. Although the FilGAP S402A mutant did not suppress cell spreading on fibronectin, localization of this mutant was not different from that of wild-type FilGAP (Fig. 4, *E* and *F*). Thus, targeting of FilGAP to the cytoskeleton may require dephosphorylation of residues other than Ser-402.

FilGAP Phosphorylated at Ser-402 Is Mainly Localized in the Cytoplasm—To study the functional significance of phosphorylation of FilGAP at Ser-402, we prepared a rabbit polyclonal antibody that specifically recognizes FilGAP protein phosphorylated at Ser-402 (anti-Ser(P)-402 antibody). The anti-Ser(P)-402 antibody recognized wild-type HA-FilGAP and the HA-FilGAP S413A mutant but not the HA-FilGAP S402A mutant (Fig. 5*A*). HA-FilGAP protein was detected when the anti-Ser(P)-402 antibody was pre-adsorbed with non-phosphorylated Ser-402 peptide but not when it was pre-adsorbed with phosphorylated peptide (Fig. 5*A*). Moreover, no signal for HA-FilGAP was detected when the protein was preincubated with calf intestine alkaline phosphatase (Fig. 5*B*). Consistent with these results, treatment of the cells with calyculin A, a phosphatase inhibitor, increased the amount of FilGAP protein recognized by the anti-Ser(P)-402 antibody (Fig. 5, *C* and *D*). Calyculin A also increased the amount of endogenous FilGAP protein recognized by the anti-Ser(P)-402 antibody (Fig. 5, *E* and *F*). Moreover, depletion of endogenous FilGAP by siRNA abolished the signal (Fig. 5, *E* and *F*). Thus, the anti-Ser(P)-402 antibody specifically recognizes endogenous FilGAP protein phosphorylated at Ser-402.

Treatment of the cells with lysophosphatidic acid and FCS increased the phosphorylation of FilGAP, which is consistent with our previous finding that phosphorylation of FilGAP is Rho/ROCK-dependent (12, 18). However, these treatments did not increase phosphorylation of Ser-402 (data not shown). Moreover, treatment of the cells with the ROCK-specific inhibitor Y27632 did not abolish phosphorylation of FilGAP at Ser-402 (Fig. 5, *G* and *H*). These results may suggest that protein kinases other than ROCK may be responsible for phosphorylation of Ser-402.

We next determined the subcellular localization of FilGAP phosphorylated at Ser-402. A7 cells were transfected with wild-type HA-FilGAP, and the Triton X-100 soluble and insoluble fractions were separated. As shown in Fig. 5, *I* and *J*, HA-FilGAP protein phosphorylated at Ser-402 was mainly found in the Triton X-100 soluble fraction. Consistent with this observation, little HA-FilGAP protein phosphorylated at Ser-402 was detected at the cytoskeleton when HA-FilGAP was transfected, and its localization was determined (Fig. 5, *K* and *L*). We also determined the localization of endogenous FilGAP protein in COS-7 cells. We detected endogenous FilGAP at the cytoskeleton, but FilGAP protein phosphorylated at Ser-402 mostly localized in the cytoplasm (Fig. 6). The localization of endogenous FilGAP seems to be specific because the fluorescent signals disappeared when the primary antibodies were pre-adsorbed with antigens.

Cell Spreading on Fibronectin Induces Dephosphorylation of FilGAP at Ser-402—We next determined whether extracellular signals such as growth factors and cell adhesion molecules reg-

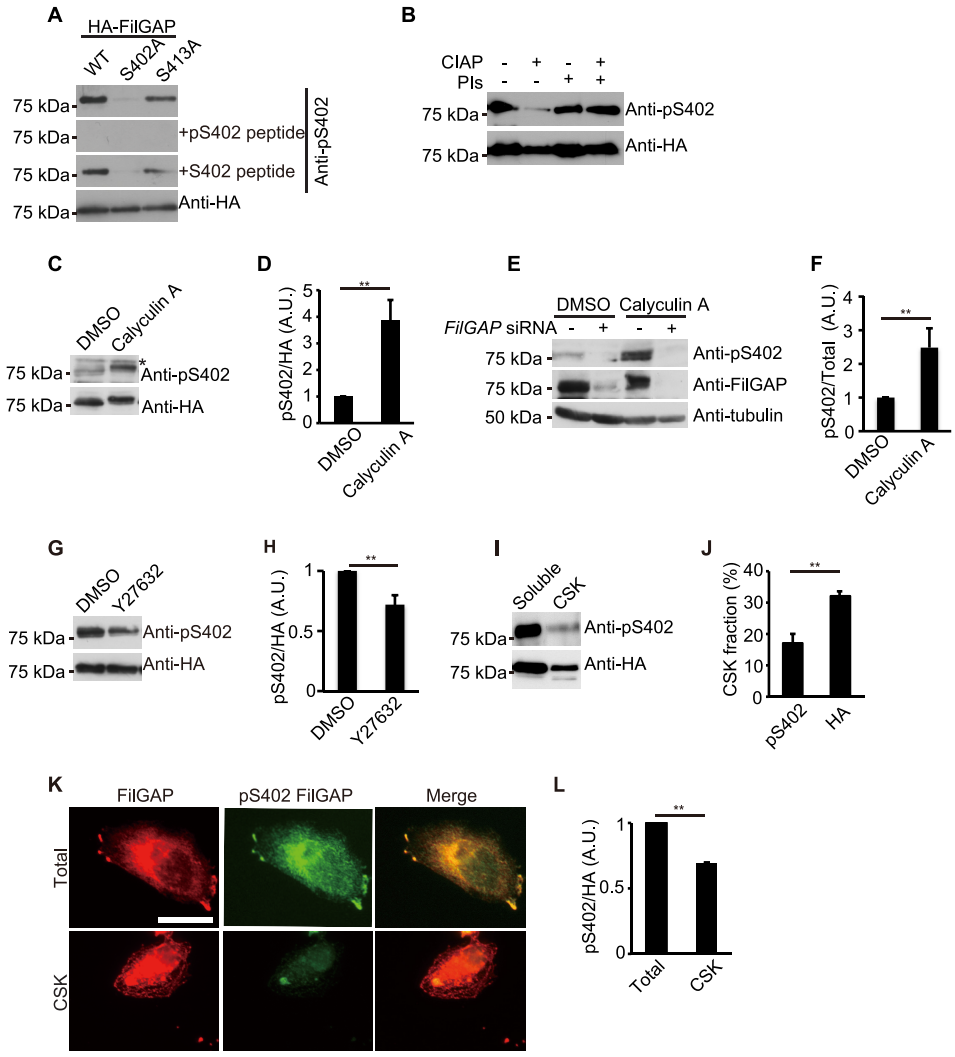

FIGURE 5. **Phosphorylation of FilGAP at serine 402 in cells.** *A*, A7 cells were transfected with HA-FilGAP constructs (wild-type, S402A, or S413A). Cell extracts were prepared and analyzed by Western blot using anti-HA or anti-Ser(P)-402 antibodies in the presence or absence of excess amounts of antigen-phosphopeptide or non-phosphopeptide. *B*, HA-FilGAP (wild-type) was isolated from transfected HEK cells using anti-HA agarose beads. The beads were washed and incubated in the presence or absence of alkaline phosphatase (*CIAP*) and phosphatase inhibitors (*PIs*) for 30 min at 37 °C. The beads were washed, and the bound FilGAP proteins were analyzed by immunoblot using anti-HA and anti-p402S FilGAP antibodies. *C*, A7 cells were transfected with HA-FilGAP (wild type) and serum-starved. Quiescent cells were incubated with DMSO or calyculin A for 30 min at 37 °C. Then cell extracts were prepared and analyzed by immunoblot using anti-HA and anti-Ser(P)-402 antibodies. *Asterisks* indicate nonspecific bands. *D*, the relative amounts of HA-FilGAP phosphorylated at Ser-402 compared with total HA-FilGAP were quantitated from digitized images of autoradiograms of immunoblots by using Image J program. Each value represents the mean ± S.E. ($n = 3$). **, $p < 0.05$. Statistical significance was determined by Student's *t* test. *A.U.*, absorbance units. *E*, COS-7 cells treated with or without *FilGAP* siRNA were serum-starved. Quiescent cells were incubated with DMSO or calyculin A for 60 min at 37 °C. Cell extracts were prepared and analyzed by Western blot using anti-FilGAP and anti-Ser(P)-402 antibodies. Tubulin was used as a loading control. *F*, the relative amounts of FilGAP phosphorylated at Ser-402 compared with total FilGAP were quantitated from digitized images of autoradiograms of immunoblots by using Image J program. Each value represents the mean ± S.E. ($n = 3$). **, $p < 0.05$. Statistical significance was determined by Student's *t* test. *G*, A7 cells were transfected with HA-FilGAP (wild type) and serum-starved. Quiescent cells were incubated with DMSO or 10 nM Y27632 for 60 min at 37 °C. Cell extracts were prepared and analyzed by Western blot using anti-HA and anti-Ser(P)-402 antibodies. *H*, the relative amounts of HA-FilGAP phosphorylated at Ser-402 compared with total HA-FilGAP was quantitated from digitized images of autoradiograms of immunoblots by using Image J program. Each value represents the mean ± S.E. ($n = 3$). **, $p < 0.05$. Statistical significance was determined by Student's *t* test. *I*, A7 cells transfected with HA-FilGAP (wild type) were lysed and Triton-solubilized, and insoluble cytoskeletal (*CSK*) fractions were prepared. Samples of each fraction were immunoblotted with anti-HA and anti-Ser(P)-402 antibodies. *J*, the relative amounts of HA-FilGAP (total protein and phosphorylated protein at Ser-402) in the cytoskeletons were quantitated from digitized images of autoradiograms of immunoblots by using Image J program. Each value represents the percentage of total and the mean ± S.E. ($n = 3$). **, $p < 0.05$. Statistical significance was determined by Student's *t* test. *K*, A7 cells transfected with HA-FilGAP (wild type) were fixed after treatment with cytoskeletal (*CSK*) or without (*Total*) 0.5% Triton X-100. HA-FilGAP (*red*) and HA-FilGAP phosphorylated at Ser-402 (*green*) were localized by staining the cells with anti-HA and anti-Ser(P)-402 antibodies. *Scale bar*, 20 μm. *L*, the relative intensities of HA-FilGAP phosphorylated at Ser-402 compared with total HA-FilGAP were calculated and plotted as the means ± S.E. ($n = 3$). **, $p < 0.01$. Statistical significance was determined by Student's *t* test.

ulate phosphorylation of FilGAP at Ser-402. We found that serum starvation of A7 cells did not significantly decrease the phosphorylation of FilGAP at Ser-402, and the addition of growth factors such as EGF did not increase the phosphorylation of FilGAP at Ser-402 (data not shown). Among the various conditions tested, spreading of cells on fibronectin induced dephosphorylation of FilGAP at Ser-402 (Fig. 7, *A* and *B*). In contrast, dephosphorylation of FilGAP at Ser-402 did not occur when the cells were plated on poly-L-lysine (Fig. 7, *A* and *B*). When cells overexpressing HA-FilGAP were plated on fibronectin and treated with calyculin A, dephosphorylation of FilGAP at Ser-402 was suppressed (Fig. 7, *C* and *D*). A7 cells

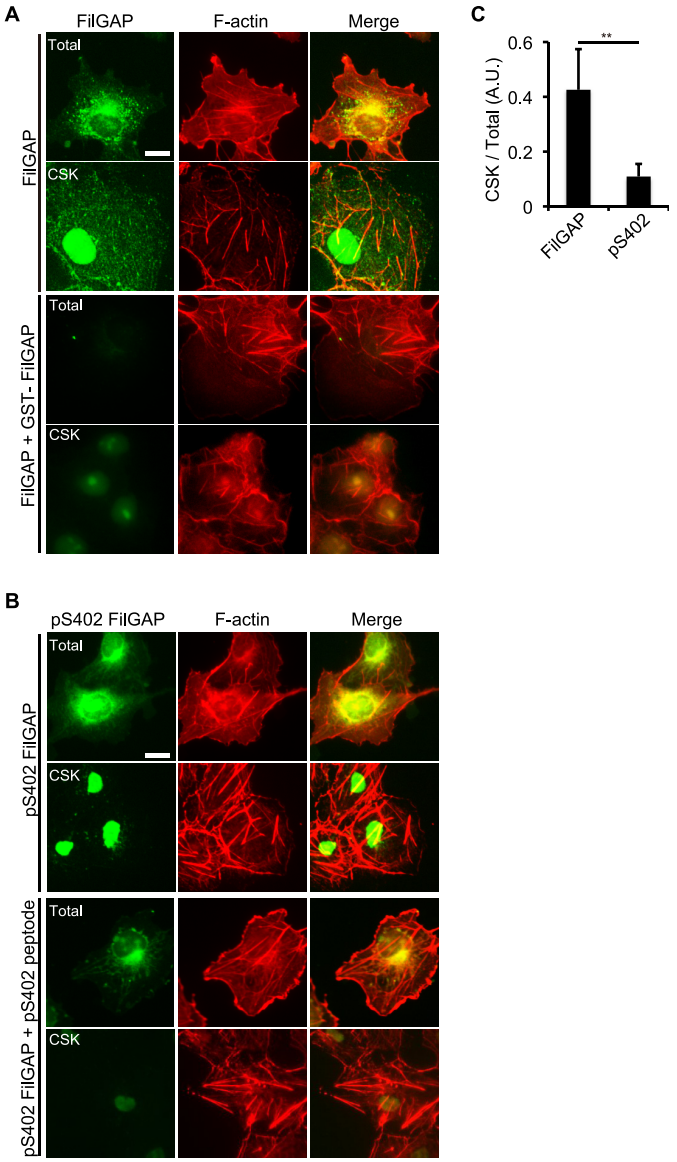

FIGURE 6. **Subcellular localization of endogenous FilGAP.** *A*, COS-7 cells were fixed after treatment with cytoskeletal (*CSK*) or without (*Total*) 0.5% Triton X-100. Then the cells were stained with anti-FilGAP antibody for endogenous FilGAP (*green*) and Alexa Fluor-phalloidin for F-actin (*red*), which were nontreated or preabsorbed with antigen (GST-FilGAP). Merged fluorescent images are also shown. *Scale bar*, 20 μm. *B*, COS-7 cells were fixed after treatment with cytoskeletal (*CSK*) or without (*Total*) 0.5% Triton X-100. Then the cells were stained with anti-Ser(P)-402 antibody for phosphorylated FilGAP (*green*) and Alexa Fluor-phalloidin for F-actin (*red*), which were nontreated or preabsorbed with antigen peptide (Ser(P)-402 peptide). Merged fluorescent images are also shown. *Scale bar*, 20 μm. *C*, the relative intensities of endogenous FilGAP (total protein and phosphorylated protein at Ser-402) in the cytoskeletons were quantitated and plotted as the means ± S.E. ($n = 3$). **, $p < 0.01$. Statistical significance was determined by Student's *t* test. *A.U.*, absorbance units.

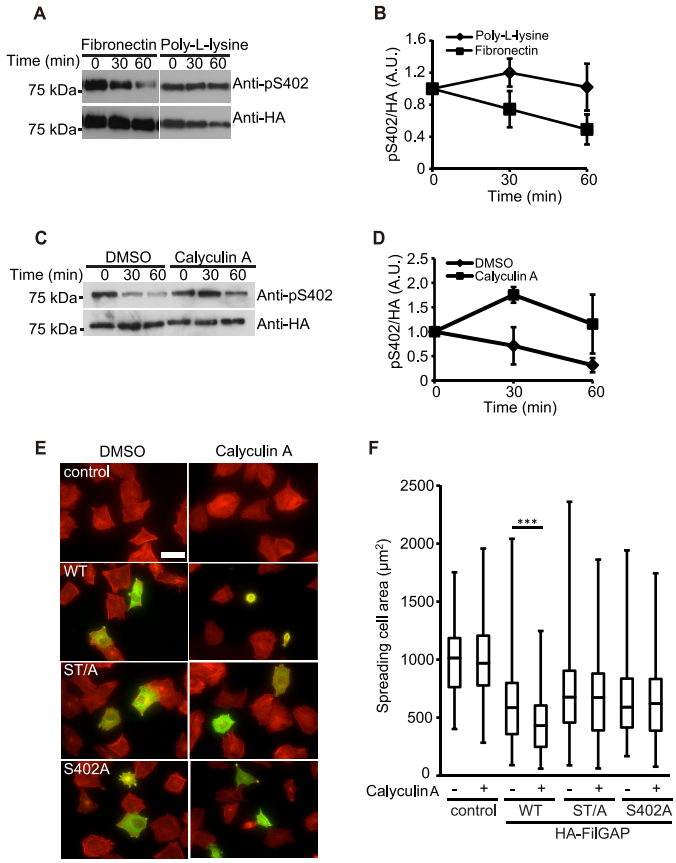

FIGURE 7. **Cell adhesion to fibronectin induces dephosphorylation of FilGAP at Serine 402.** *A*, A7 cells were transfected with HA-FilGAP (wild type) and serum-starved. Quiescent cells were trypsinized, and cells in suspension were plated on dishes coated with fibronectin or poly-L-lysine for the indicated times. Cell extracts were prepared and analyzed by Western blot using anti-HA and anti-Ser(P)-402 antibodies. *B*, the relative amounts of FilGAP protein phosphorylated at Ser-402 were calculated and plotted as the mean ± S.E. ($n = 3$). *A.U.*, absorbance units. *C*, A7 cells were transfected with HA-FilGAP (wild type) and serum-starved. Quiescent cells were incubated with DMSO or 10 nM calyculin A for 30 min at 37 °C. Then the cells were trypsinized, and cells in suspension were plated on dishes coated with fibronectin or poly-L-lysine for the indicated times. Cell extracts were prepared and analyzed by Western blot using anti-HA and anti-Ser(P)-402 antibodies. *D*, the relative amount of FilGAP protein phosphorylated at Ser-402 was calculated and plotted as the mean ± S.E. ($n = 3$). *E*, A7 cells were transfected with HA-FilGAP constructs (*WT*, *ST/A*, or *S402A*) and serum-starved. Quiescent cells were incubated with DMSO or calyculin A for 30 min at 37 °C. Then the cells were trypsinized, and cells in suspension were plated on coverslips coated with fibronectin and fixed 20 min after plating. Cells were stained with anti-HA antibody (*green*) and Alexa Fluor-phalloidin (*red*). *Scale bar*, 40 μm. *F*, the surface area of spreading cells 60 min after plating was calculated and plotted as the mean ± S.E. ($n = 3$). >50 cells were counted in each experiment. ***, $p < 0.005$. Statistical significance was determined by one-way ANOVA.

plated on fibronectin-coated dishes spread and achieved a maximal extent flattening by 1 h (Fig. 7*E*). Treatment of control A7 cells with calyculin A did not affect cell spreading or flattening on fibronectin (Fig. 7, *E* and *F*). However, calyculin A treatment of A7 cells overexpressing wild-type FilGAP suppressed cell spreading on fibronectin, whereas spreading of A7 cells overexpressing FilGAP mutants (ST/A and S402A) was not affected by calyculin A (Fig. 7, *E* and *F*). Thus, dephosphorylation of FilGAP at Ser-402 may be necessary for efficient spreading on fibronectin.

We confirmed that dephosphorylation of endogenous FilGAP could be induced by cell spreading on fibronectin. The amount of FilGAP phosphorylated at Ser-402 in COS-7 cells as detected by immunofluorescent staining was reduced after the cells were plated on fibronectin (Fig. 8).

Regulation of Plasma Membrane Blebbing by Arf6 and Phosphorylation of FilGAP—We previously showed that Arf6 GTPase binds to FilGAP and stimulates its RacGAP activity to induce plasma membrane blebbing (20). We examined whether Arf6-mediated regulation has any role in the phosphorylation-

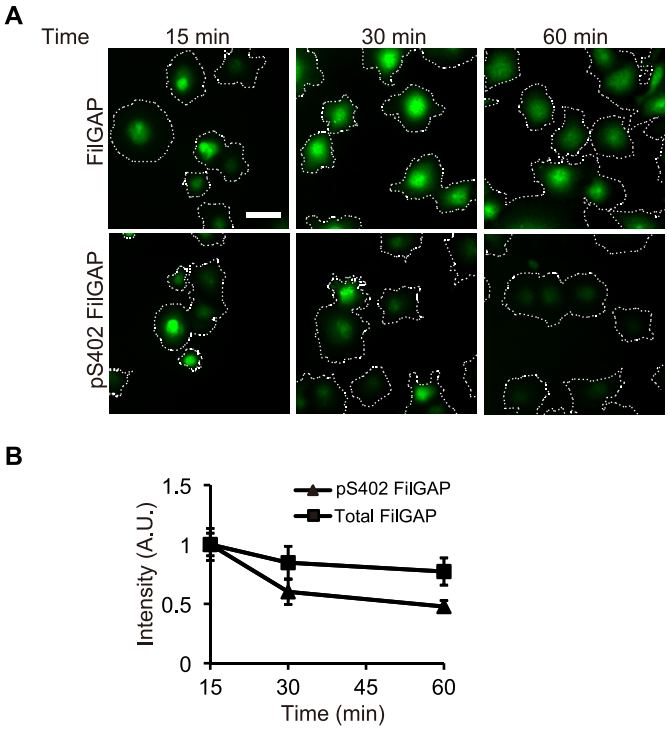

FIGURE 8. **Cell adhesion to fibronectin induces dephosphorylation of endogenous FilGAP at serine 402.** COS-7 cells were serum-starved. Quiescent cells were trypsinized, and cells in suspension were plated on coverslips coated with fibronectin for the indicated time periods. Cells were fixed and stained with anti-FilGAP or anti-Ser(P)-402 antibodies. *Dotted lines* indicate cell peripheries. *Scale bar*, 40 μm. B, the relative intensities of p402S FilGAP compared with total FilGAP were calculated and plotted as the means ±S.E. ($n = 3$). *A.U.*, absorbance units.

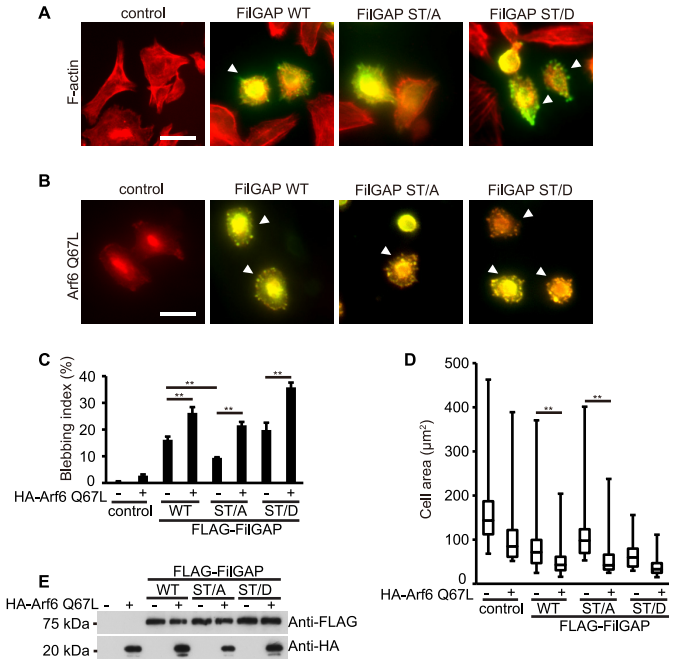

FIGURE 9. **Arf6 and phosphorylation of FilGAP regulate bleb formation.** *A*, A7 cells were transfected with FLAG-FilGAP constructs (*WT*, *ST/A*, and *ST/D*). After 24 h the cells were fixed and stained with anti-FLAG antibody for FLAG-FilGAP (*green*) and Alexa Fluor-phalloidin for F-actin (*red*). *Scale bar*, 40 μm. *Arrowheads* indicate the membrane blebbing cells. *B*, A7 cells were transfected with FLAG-FilGAP constructs (*WT*, *ST/A*, and *ST/D*) in the presence of constitutively activated HA-Arf6 Q67L. After 24 h, the cells were fixed and stained with anti-FLAG antibody for FLAG-FilGAP (*green*) and anti-HA antibody for Arf6 Q67L (*red*). *Scale bar*, 40 μm. *Arrowheads* indicate the membrane blebbing cells. *C*, the percentage of blebbing cells was calculated, and the data are expressed as the mean = S.E. ($n = 3$). **, $p < 0.01$. Statistical significance was determined by one-way ANOVA. *D*, the surface area of cells was calculated and plotted as the mean ± S.E. ($n = 3$). **, $p < 0.01$. Statistical significance was determined by one-way ANOVA. *E*, A7 cells were transfected with FLAG-FilGAP and HA-Arf6 Q67L. Cell extracts were prepared and analyzed by Western blot using anti-HA and anti-FLAG antibodies.

dependent activation of FilGAP. Forced expression of FilGAP in A7 cells induced membrane blebbing around the cell periphery (Fig. 9, *A* and *C*). The non-phosphorylatable FilGAP (ST/A) mutant failed to induce blebbing, whereas the phosphomimetic FilGAP (ST/D) mutant induced blebbing as efficiently as wild-type FilGAP (Fig. 9, *A* and *C*).

Forced expression of the constitutively activated mutant Arf6 Q67L stimulated plasma membrane blebbing induced by wild-type FilGAP (Fig. 9, *B* and *C*). Arf6 Q67L also stimulated both phosphomimetic (ST/D) FilGAP and non-phosphorylatable (ST/A) FilGAP activity (Fig. 9, *B* and *C*). The smaller spreading area of cells expressing Arf6 Q67L also suggested that Arf6 stimulates FilGAP activity, because cell area is reduced by the contraction of blebbing cells (Fig. 9*D*). We further examined the role of Arf6 using *Arf6* siRNA. Depletion of endogenous Arf6 by siRNA suppressed bleb formation induced by both wild-type and phosphomimetic (ST/D) FilGAP mutant (Fig. 10, *A* and *C*). Knockdown of endogenous Arf6 suppressed cell shrinkage induced by overexpression of wild-type as well as the ST/A and ST/D mutants (Fig. 10*D*). We generated a construct resistant to Arf6 siRNA (HA-Arf6 Q67L^R) and examined whether down-regulation of FilGAP activity by Arf6 siRNA was prevented. At 48 h after transfection with Arf6 siRNA, HA-Arf6 Q67L^R, but not endogenous Arf6 protein, was abundantly expressed in A7 cells (Fig. 10*E*), and HA-Arf6 Q67L^R rescued the induction of membrane blebbing by wild-type and phosphomimetic FilGAP (ST/D) (Fig. 10, *B* and *C*). Thus, Arf6-mediated regulation of FilGAP may be distinct from phosphorylation-dependent activation of FilGAP.

Discussion

In this study we demonstrated that FilGAP is localized to the cytoskeleton and cytoplasm and that phosphorylation of FilGAP may induce translocation of the protein from the cytoskeleton to the cytoplasm to activate its RacGAP activity. We identified Ser-402 as a critical phosphorylation site for the activation of FilGAP to suppress cell spreading on fibronectin.

Several lines of evidence suggest that phosphorylation of FilGAP may regulate its subcellular localization. First, >40% of the non-phosphorylatable FilGAP (ST/A) mutant was found in the Triton X-100 insoluble fraction (the cytoskeleton), and this mutant localized with actin filaments and partially co-localized with the focal adhesion protein vinculin. In contrast, the phosphomimetic FilGAP (ST/D) mutant was found in the Triton X-100 soluble fraction and barely detectable at the cytoskeleton by immunofluorescent staining. Second, much of the phosphorylated FilGAP protein detected in Phos-tag SDS-PAGE was present in the Triton X-100 soluble fraction. Moreover, treatment of the cells with calyculin A reduced the amount of FilGAP protein localized to the cytoskeleton. We showed previously that Rho/ROCK-dependent

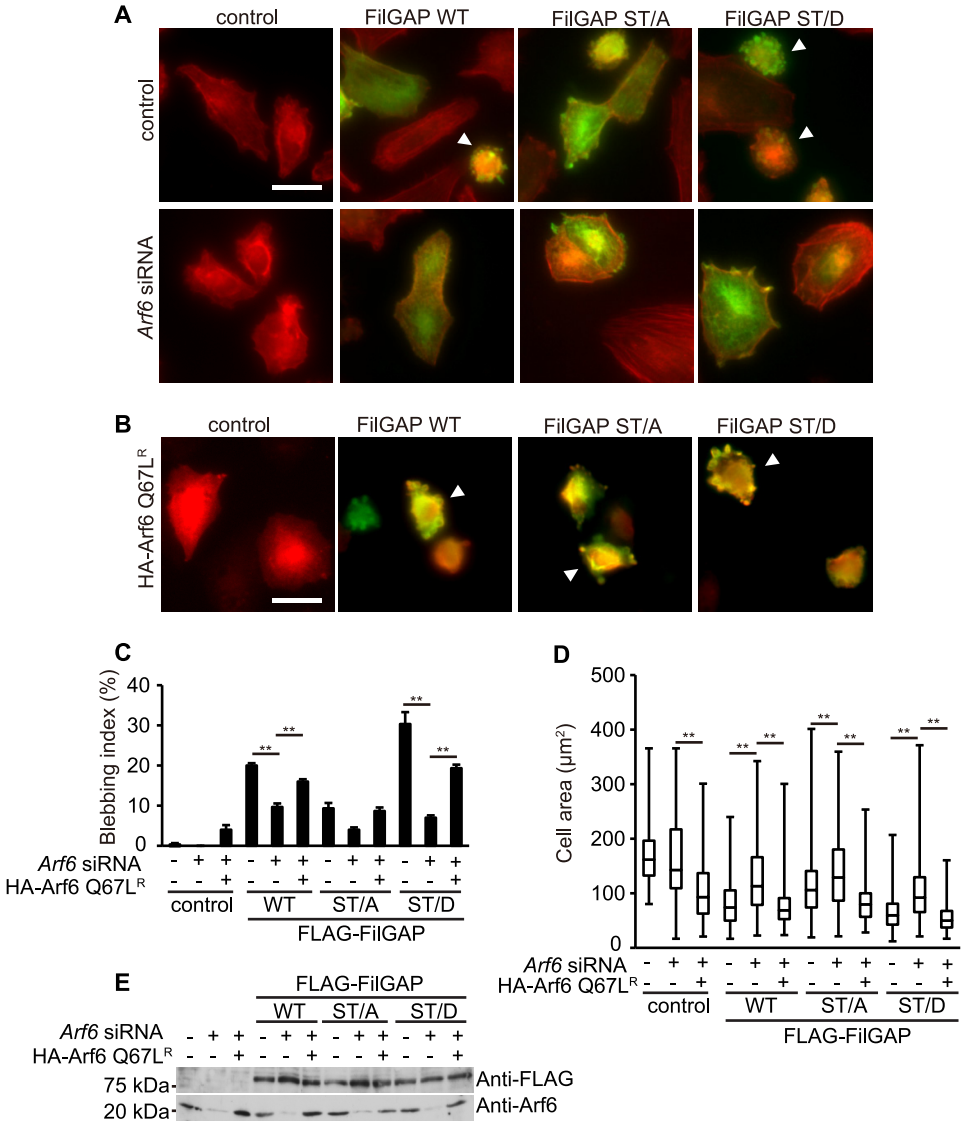

FIGURE 10. **Depression of Arf6 suppressed bleb formation induced by phosphorylation of FilGAP.** *A*, A7 cells were treated with or without *Arf6* siRNA in the absence or presence of FLAG-FilGAP constructs. For co-transfection of plasmid DNA and *Arf6* siRNA, the cells were first transfected with siRNA for 24 h and then cotransfected with plasmid DNA. After 24 h, cells were fixed and stained with anti-FLAG antibody for FLAG-FilGAP (*green*) and Alexa Fluor-phalloidin for F-actin (*red*). Representative merged images are shown. *Scale bar*, 40 μm. *Arrowheads* indicate the membrane blebbing cells. *B*, A7 cells were transfected with *Arf6* siRNA for 24 h and then co-transfected with FLAG-FilGAP constructs and HA-Arf6 Q67L resistant to *Arf6* siRNA (*HA-Arf6 Q67L^R*). After 24 h, cells were fixed and stained with anti-FLAG antibody for FLAG-FilGAP (*green*) and anti-HA antibody for Arf6 Q67L^R (*red*). Representative merged images are shown. *Scale bar*, 40 μm. *Arrowheads* indicate the membrane blebbing cells. *C*, the percentage of blebbing cells was calculated, and the data are expressed as the mean $\pm$ S.E. ($n = 3$). Statistical significance was determined by one-way ANOVA. **, $p < 0.01$. *D*, the surface area of cells was calculated and plotted as the mean $\pm$ S.E. ($n = 3$). **, $p < 0.01$. Statistical significance was determined by one-way ANOVA. *E*, A7 cells were transfected with FLAG-FilGAP with or without *Arf6* siRNA. Cell extracts were prepared and analyzed by Western blot using anti-FLAG and anti-Arf6 antibodies.

phosphorylation of FilGAP stimulates its RacGAP activity, but how phosphorylation regulates FilGAP remains unclear (12). It is possible that the phosphorylation-dependent release of FilGAP from the cytoskeleton induces translocation of FilGAP to the plasma membrane to inactivate Rac. This is consistent with our finding that bleb formation induced by FilGAP requires the pleckstrin homology domain, which binds to the plasma membrane (20).

Of the six potential phosphorylation sites in FilGAP, Ser-402 seems to be important for the protein's activity. Among the FilGAP mutants with one potential phosphorylation site mutated to alanine, only S402A failed to suppress cell spreading on fibronectin. This is consistent with our previous finding that S402A was the least effective in inducing membrane blebbing (12). However, our present study suggests that phosphorylation of Ser-402 may not be responsible for release of FilGAP from the cytoskeleton. FilGAP protein phosphorylated at Ser-402 is mostly localized in the cytoplasm as detected by anti-Ser(P)-402 antibody. However, we found that localization of the non-phosphorylatable FilGAP S402A mutant was not different from that of wild-type FilGAP. Therefore, translocation of FilGAP from the cytoskeleton to the cytoplasm may be induced by phosphorylation of sites in FilGAP other than Ser-402. Phosphorylation of FilGAP at Ser-402 may regulate FilGAP activity through an as yet unidentified mechanism other than release of FilGAP from the cytoskeleton.

Although FilGAP is phosphorylated downstream of Rho/ROCK signaling, our present study suggests that ROCK may not be the principal protein kinase responsible for phosphorylation of FilGAP at Ser-402. We found that serum starvation of A7 cells did not significantly decrease the phosphorylation of FilGAP at Ser-402, and stimulation with agonists such as lysophosphatidic acid and EGF did not increase the phosphorylation of FilGAP at Ser-402. Moreover, treatment of cells with the ROCK-specific inhibitor Y27632 did not diminish the phosphorylation of Ser-402. Thus, Rho/ROCK-dependent phosphorylation of multiple sites other than Ser-402 may induce translocation of FilGAP from the cytoskeleton to activate its RacGAP activity. FilGAP protein phosphorylated at Ser-402 was mostly detected in the cytoplasm; therefore, Ser-402 may be phosphorylated in the cytoplasm after FilGAP is translocated from the cytoskeleton. Ser-402 matches the consensus phosphorylation sequence defined for various protein kinases, and therefore, multiple kinases may be responsible for phosphorylation of Ser-402 (25–27).

Cell spreading on extracellular matrix such as fibronectin initiates complex arrays of signaling through activation of integrin (28–32). We found that cell spreading on fibronectin induced dephosphorylation of Ser-402, which may have a physiological significance. Forced expression of wild-type FilGAP suppressed initial cell spreading on fibronectin and maximal flattening was attained by 1 h. Treatment of the cells with calyculin A, a phosphatase inhibitor, further suppressed cell flattening on fibronectin, suggesting that dephosphorylation of Ser-402 may occur downstream of integrin activation. However, calyculin A treatment of cells expressing the S402A mutant did not affect cell spreading on fibronectin. Therefore, dephosphorylation of Ser-402 may be necessary and sufficient for inactivation of FilGAP to induce maximal flattening. Previous studies have suggested that protein serine/threonine phosphatases are involved in the control of cell spreading on fibronectin (33–36). Our present study suggests that dephosphorylation of endogenous FilGAP at Ser-402 may occur during cell spreading on fibronectin. It is necessary to determine whether dephosphorylation of Ser-402 of endogenous FilGAP has any role in the control of integrin-dependent cell spreading.

RhoGAPs are multidomain proteins that are regulated downstream of distinct signaling cascades (7). Activated Arf6 recruits FilGAP to plasma membrane and stimulates its RacGAP activity (20). Our present study suggests that Arf6 and phosphorylation of FilGAP may independently regulate FilGAP to stimulate its RacGAP activity. Forced expression of the constitutively activated mutant Arf6 Q67L stimulated not only wild-type FilGAP and the phosphomimetic FilGAP (ST/D) mutant but also non-phosphorylatable FilGAP (ST/A) mutant. Conversely, depletion of endogenous Arf6 by siRNA suppressed plasma membrane blebbing induced by the phosphomimetic (ST/D) and non-phosphorylatable (ST/A) FilGAP mutants. This may be consistent with our model in which activated Arf6 at the plasma membrane recruits FilGAP by binding its pleckstrin homology domain, allowing FilGAP to inactivate Rac at the membrane. Phosphorylation of FilGAP may induce translocation of FilGAP from the cytoskeleton to the cytoplasm increasing FilGAP access to the plasma membrane. It remains to be determined how phosphorylation of Ser-402 is involved in the activation of FilGAP. Phosphorylation of Ser-402 may be required for release of an as yet unidentified inhibitor from FilGAP. Further study is necessary to understand the mechanism of regulation.

In conclusion, our study demonstrated that dephosphorylation of FilGAP occurs during integrin-mediated cell adhesion on fibronectin. Both integrin-mediated protein phosphorylation and integrin-mediated protein dephosphorylation may play a role in the control of Rho GTPase signaling.

Author Contributions—Y. M., K. T., and Y. O. designed the study and wrote the paper. Y. M. performed and analyzed the experiments. All authors reviewed the results and approved the final version of the manuscript.

Acknowledgment—We thank Y. Nakazawa for help in preparation of anti-Ser(P)-402 antibody.

References

1. Burridge, K., and Wennerberg, K. (2004) Rho and Rac take center stage. *Cell* **116,** 167–179
2. Jaffe, A. B., and Hall, A. (2005) Rho GTPases: Biochemistry and biology. *Annu. Rev. Cell Dev. Biol.* **21,** 247–269
3. Heasman, S. J., and Ridley, A. J. (2008) Mammalian Rho GTPases: new insights into their functions from *in vivo* studies. *Nat. Rev. Mol. Cell Biol.* **9,** 690–701
4. Parsons, J. T., Horwitz, A. R., and Schwartz, M. A. (2010) Cell adhesion: integrating cytoskeletal dynamics and cellular tension. *Nat. Rev. Mol. Cell Biol.* **11,** 633–643
5. Hall, A. (2012) Rho family GTPases. *Biochem. Soc. Trans.* **40,** 1378–1382
6. Sadok, A., and Marshall, C. J. (2014) Rho GTPases: masters of cell migration. *Small GTPases* **5,** e29710
7. Bos, J. L., Rehmann, H., and Wittinghofer, A. (2007) GEFs and GAPs: critical elements in the control of small G proteins. *Cell* **129,** 865–877
8. McCormack, J., Welsh, N. J., and Braga, V. M. (2013) Cycling around cell-cell adhesion with Rho GTPase regulators. *J. Cell Sci.* **126,** 379–391
9. Miller, N. L., Kleinschmidt, E. G., and Schlaepfer, D. D. (2014) RhoGEFs in cell motility: novel links between Rgnef and focal adhesion kinase. *Curr. Mol. Med.* **14,** 221–234
10. Cook, D. R., Rossman, K. L., and Der, C. J. (2014) Rho guanine nucleotide exchange factors: regulators of Rho GTPase activity in development and disease. *Oncogene* **33,** 4021–4035
11. van Buul, J. D., Geerts, D., and Huveneers, S. (2014) Rho GAPs and GEFs: controling switches in endothelial cell adhesion. *Cell Adh. Migr.* **8,** 108–124
12. Ohta, Y., Hartwig, J. H., and Stossel, T. P. (2006) FilGAP, a Rho- and ROCK-regulated GAP for Rac binds filamin A to control actin remodelling. *Nat. Cell Biol.* **8,** 803–814
13. Nakamura, F., Osborn, T. M., Hartemink, C. A., Hartwig, J. H., and Stossel, T. P. (2007) Structural basis of filamin A functions. *J. Cell Biol.* **179,** 1011–1025
14. Shifrin, Y., Arora, P. D., Ohta, Y., Calderwood, D. A., and McCulloch, C. A. (2009) The role of FilGAP-filamin A interactions in mechanoprotection. *Mol. Biol. Cell* **20,** 1269–1279
15. Nakamura, F., Heikkinen, O., Pentikäinen, O. T., Osborn, T. M., Kasza, K. E., Weitz, D. A., Kupiainen, O., Permi, P., Kilpeläinen, I., Ylänne, J., Hartwig, J. H., and Stossel, T. P. (2009) Molecular basis of filamin A-FilGAP interaction and its impairment in congenital disorders associated with filamin A mutations. *PLoS ONE* **4,** e4928
16. Nieves, B., Jones, C. W., Ward, R., Ohta, Y., Reverte, C. G., and LaFlamme, S. E. (2010) The NPIY motif in the integrin beta 1 tail dictates the requirement for talin-1 in outside-in signaling. *J. Cell Sci.* **123,** 1216–1226
17. Ehrlicher, A. J., Nakamura, F., Hartwig, J. H., Weitz, D. A., and Stossel, T. P.

(2011) Mechanical strain in actin networks regulates FilGAP and integrin binding to filamin A. *Nature* **478,** 260–263
18. Saito, K., Ozawa, Y., Hibino, K., and Ohta, Y. (2012) FilGAP, a Rho/Rho-associated protein kinase-regulated GTPase-activating protein for Rac, controls tumor cell migration. *Mol. Biol. Cell* **23,** 4739–4750
19. Nakamura, F. (2013) FilGAP and its close relatives: a mediator of Rho-Rac antagonism that regulates cell morphology and migration. *Biochem. J.* **453,** 17–25
20. Kawaguchi, K., Saito, K., Asami, H., and Ohta, Y. (2014) ADP ribosylation factor 6 (Arf6) acts through FilGAP protein to down-regulate Rac protein and regulates plasma membrane blebbing. *J. Biol. Chem.* **289,** 9675–9682
21. Guilluy, C., Garcia-Mata, R., and Burridge, K. (2011) Rho protein crosstalk: another social network? *Trends Cell Biol.* **21,** 718–726
22. Petrie, R. J., and Yamada, K. M. (2012) At the leading edge of three-dimensional cell migration. *J. Cell Sci.* **125,** 5917–5926
23. Kinoshita, E., and Kinoshita-Kikuta, E. (2011) Improved Phos-tag SDS-PAGE under neutral pH conditions for advanced protein phosphorylation profiling. *Proteomics* **11,** 319–323
24. Kinoshita-Kikuta, E., Aoki, Y., Kinoshita, E., and Koike, T. (2007) Label-free kinase profiling using phosphate affinity polyacrylamide gel electrophoresis. *Mol. Cell. Proteomics* **6,** 356–366
25. Riento, K., and Ridley, A. (2003) ROCKS: multifunctional kinases in cell behaviour. *Nat. Rev. Mol. Cell Biol.* **4,** 446–456
26. Huang, C., Jacobson, K., and Schaller, M. (2004) MAP kinases and cell migration. *J. Cell Sci.* **117,** 4619–4628
27. Etienne-Manneville, S., and Hall, A. (2003) Cdc42 regulates GSK-3beta and adenomatous polyposis coli to control cell polarity. *Nature* **421,** 753–756
28. Tomar, A., and Schlaepfer, D. D. (2009) Focal adhesion kinase: switching between GAPs and GEFs in the regulation of cell motility. *Curr. Opin. Cell Biol.* **21,** 676–683
29. Huveneers, S., and Danen, E. H. (2009) Adhesion signaling: crosstalk between integrins, Src and Rho. *J. Cell Sci.* **122,** 1059–1069
30. Wolfenson, H., Lavelin, I., and Geiger, B. (2013) Dynamic regulation of the structure and functions of integrin adhesions. *Dev. Cell* **24,** 447–458
31. Winograd-Katz, S. E., Fässler, R., Geiger, B., and Legate, K. R. (2014) The integrin adhesome: from genes and proteins to human disease. *Nat. Rev. Mol. Cell Biol.* **15,** 273–288
32. Lawson, C. D., and Burridge, K. (2014) The on-off relationship of Rho and Rac during integrin-mediated adhesion and cell migration. *Small GTPases* **5,** e27958
33. Bianchi, M., De Lucchini, S., Marin, O., Turner, D. L., Hanks, S. K., and Villa-Moruzzi, E. (2005) Regulation of FAK Ser-722 phosphorylation and kinase activity by GSK3 and PP1 during cell spreading and migration. *Biochem. J.* **391,** 359–370
34. Kiely, P. A., O'Gorman, D., Luong, K., Ron, D., and O'Connor, R. (2006) Insulin-like growth factor I controls a mutually exclusive association of RACK1 with protein phosphatase 2A and beta1 integrin to promote cell migration. *Mol. Cell. Biol.* **26,** 4041–4051
35. Kong, M., Bui, T. V., Ditsworth, D., Gruber, J. J., Goncharov, D., Krymskaya, V. P., Lindsten, T., and Thompson, C. B. (2007) The PP2A-associated protein alpha4 plays a critical role in the regulation of cell spreading and migration. *J. Biol. Chem.* **282,** 29712–29720
36. Hall, E. H., Daugherty, A. E., Choi, C. K., Horwitz, A. F., and Brautigan, D. L. (2009) Tensin1 requires protein phosphatase-1alpha in addition to RhoGAP DLC-1 to control cell polarization, migration, and invasion. *J. Biol. Chem.* **284,** 34713–34722